興大工程學報 第八卷 第二期 (民國八十六年六月)
Journal of Engineering, National Chung Hsing University, Vol. 8, No. 2, pp. 21-29 (1997).

AN OBSERVATION OF OXYGEN PRECIPITATION RETARDATION PHENOMENON INDUCED BY 450℃ ANNEAL IN CZOCHRALSKI SILICON

C.Y. Kung[1], W. Hsu[2] and J.M. Liu[2]

Department of Electrical Engineering
National Chung-Hsing University
Taichung, Taiwan 40227, R.O.C.

Key Word: Oxygen precipitate, Precipitation retardation, Rod-like defect, Three-step anneal, Two-step anneal, Silicon.

ABSTRACT

Two-step (450℃-1000℃) and three-step (1150℃-450℃-1000℃) annealing experiments were carried out to study oxygen precipitation behavior in Czochralski silicon. A distinct retardation of precipitation was observed during the two-step anneal, while the retardation during the three-step anneal was less pronounced. With the three-step anneal, the first high temperature 1150℃ anneal in N_2 ambient caused the retardation to occur at shorter nucleation times. The microstructure characteristics as a function of nucleation (450℃) anneal time were similar in the two-step and three-step annealed samples.

450℃ 退火對 Cz 矽晶內氧凝聚遲滯現象所造成的影響

貢中元[1] 徐瑋[2] 劉進明[2]

關鍵詞：氧凝聚遲滯、氧凝聚物、二溫階退火、三溫階退火、微觀結構。

摘 要

本文以二溫階 (450℃-1000℃) 和三溫階 (1150℃-450℃-1000℃) 退火實驗來研究 Cz 矽晶內的氧凝聚行爲。在二溫階的實驗中觀察到很明顯的氧凝聚遲滯現象，然而在三溫階實驗中氧凝聚遲滯現象則不明顯。在三溫階實驗第一步驟 1150℃的高溫退火，會使氧凝聚遲滯現象在較短的孕核時間內發生。我們發現矽晶內的微觀缺陷隨著 450 ℃的孕核時間而改變。二溫階與三溫階退火所產生的微觀缺陷隨 450℃退火時間的變化是十分類似的。

[1] 國立中興大學電機系教授
[2] 國立中興大學材料所研究生

1. INTRODUCTION

Oxygen precipitation in Cz silicon has been an interesting topic because the oxide recipitates are found to have a gettering effect [1]; a high density of oxide precipitates in the bulk of the wafer with an appropriate denuded zone free of such precipitates near the wafer surface can benefit the device characteristics. Two-step[2-4] (low-high) and three-step[5,6] (high-low-high) annealing processes are applied in order to provide the best conditions for integrated circuit fabrication. In the two-step anneal, the low temperature step is utilized for precipitate nucleation and the subsequent high temperature step is for precipitate growth. From the metallurgical point of view, a longer nucleation anneal should generate more precipitate nuclei and result in a faster precipitate growth during the subsequent high temperature anneal. However, in a study of two-step (700℃-1000℃) annealing in dry O_2 ambient, Ogino[7] first observed that the oxide precipitate growth rate decreases with increasing low temperature nucleation anneal time. This phenomenon is called low-temperature-induced precipitation retardation. Ogino observed that the retardation occurred in wafers with high carbon concentration that had been annealed for 64 h at 700℃, but not in wafers with low carbon concentration.

Kung, Forbes, and Peng [8]; Tan and Kung [9] and Kung[10] have extensively studied low-temperature-induced precipitation retardation during two-step annealing (650℃/750℃-1050℃) in N_2 ambient. They observed that for certain wafers, retardation occurred during two-step annealing when the wafers were annealed at 750℃ for 2 to 16 h. For some other wafers, retardation was not observed during the 750℃-1050℃ two-step process, but was observed during a two-step process when the wafers were annealed at 650℃ for 32 to 64 h. Kung [8,10] observed that a short wet oxidation at 1000℃ prior to the two-step anneal eliminated the retardation effect. It should be noted that, although it was not reported explicitly in these experiments [8-10], the wafers were ramped up to high temperature (1000℃ or 1050℃) at a rate of 8℃/min and ramped down at a rate of 5℃/min in accordance with standard operating procedures in place in the Fairchild laboratory at the time of the experiments.

Several models have been proposed to explain the precipitation phenomenon; these were reviewed by Tan and Kung[9]. Among these models, the silicon interstitial (I) supersaturation model proposed by Tan and Kung is the most convincing. Rogers et al.[11] have conducted a refined experiment that supports the I-supersaturation model; they suggest that nuclei dissolution induced by I supersaturation occurred during temperature ramping at the precipitate growth stage.

To understand more about precipitation retardation, we conducted similar two-and three-step experiments, choosing 450℃ as the nucleation anneal temperature. Rod-like defects which are the key factor in the I-supersaturation model are found after prolonged annealing at both 650℃ and 450℃ [12,13].The annealing time at 450℃ needed to reveal rod-like defects is much longer than that at 650℃. It was expected that precipitation retardation would occur in the samples which received longer annealing at 450℃ during the two-step (450℃-1000℃) anneal test. Therefore, in this research, we extended the 450℃ anneal time up to 1024 h. We also performed the growth anneal (1000℃) with fast heating up and cooling down rates in order to determine whether ramping influenced the occurrence of precipitate retardation. The result shows that even in the absence of ramping, precipitation retardation occurred during the two-step anneal. It was found that the annealing time at 450℃ needed to induce precipitation retardation was between about 16 h and about 128 h in the two-step anneal; this is about the same as the time needed to induce precipitation retardation in a 650℃-1050℃ two-step test [10].

2. EXPERIMENTAL

Several 150-mm, p-type, (100), commercially obtained, Cz wafers were chosen from the same box. The interstitial oxygen concentration in these wafers was between 14.1 ppma and 14.4 ppma (new ASTM*) and the room-temperature resistivity was between 40Ω and 45Ω-cm. These wafers are assumed to have come from the same part of an ingot and are therefore expected to have identical precipitation characteristics. To conduct the experiment, each wafer was cleaved into several parts; some parts were given two-step anneals and other, adjacent, parts were given three-step anneals. In the two-step anneal, the low-temperature nucleation anneal was conducted at 450℃ for 0 h to 1024 h. The second high temperature growth anneal was conducted at 1000℃. The cumulative anneal time was 1 min, 2 min, 5 min, 10 min, 30 min, 1 h, 2 h, 4 h, 8 h, 16 h, 24 h, 32 h and 40h. The early stage precipitation behavior was determined from the results obtained after short anneal times (up to 2 h).

The three-step anneal cycles consisted of two-step anneal cycles as described above preceded by a 1-h heat treatment at 1150℃. All anneals were carried out in a dry N_2 ambient. To avoid possible effects induced by ramping to the high temperatures (1000℃ and 1150℃), the samples were pushed rapidly into a furnace pre-heated to the anneal temperature. After the anneal time, the samples were pulled out from the furnace and cooled down rapidly to room temperature in air. The oxygen concentration of each sample was measured after each anneal step by Fourier transform infrared spectrometry in accordance with ASTM Test Method F 121-83. After the final growth anneal step (40 h cumulative anneal), the samples were cleaved and etched in Wright etchant[14] for 3 min to reveal the defect microstructure for examination by optical and scanning electron microscopy.

* The interstitial oxygen concentration, in parts per million atomic (ppma) on this scale is 4.9α, where α is the measured absorption coefficient at a wavenumber of 1107 cm^{-1}.

3. RESULTS AND DISCUSSION

Figure 1 shows the interstitial oxygen concentration in the samples as a function of nucleation anneal time at 450℃ for selected growth anneal times at 1000℃. Results are shown for both two-step and three-step anneal cycles. The difference between this oxygen concentration and the initial oxygen concentration in the sample is equal to the amount of oxygen precipitated.

We first discuss the results for the 450℃ nucleation anneals shorter than 256 h. In the samples given a two-step anneal, a precipitation retardation and recovery effect[9] can clearly be seen for samples that were annealed at 1000℃ for 16 h, 32 h, and 40 h. Samples that received nucleation anneals for 32 h and 64 h have higher post-growth anneal oxygen concentration than samples that received nucleation anneals for shorter times (8 h and 16 h). Thus precipitation was retarded in the samples that received nucleation anneals for 32 h and 64 h. Samples that received nucleation anneals of 128h and longer showed rapid oxygen precipitation at 1000℃, indicating a precipitation recovery effect. In the samples that received three-step anneals, the retardation effect is less pronounced, but it can be seen that samples received nucleation anneals for 8h and 16 h had higher post-growth anneal oxygen concentration than the sample that received no nucleation anneal.

By comparing the post-growth oxygen concentrations of the as-received wafers (two-step with no nucleation anneal) and wafers pre-annealed for 1 h at 1150℃ (three-step anneal) for short (1 h or less) growth anneals in Fig. 1(a) and Fig. 1(b), respectively, it can be readily seen that the 1150℃ anneal does not affect either the oxygen nucleation rate or the agglomeration rate at 450℃. Oxygen

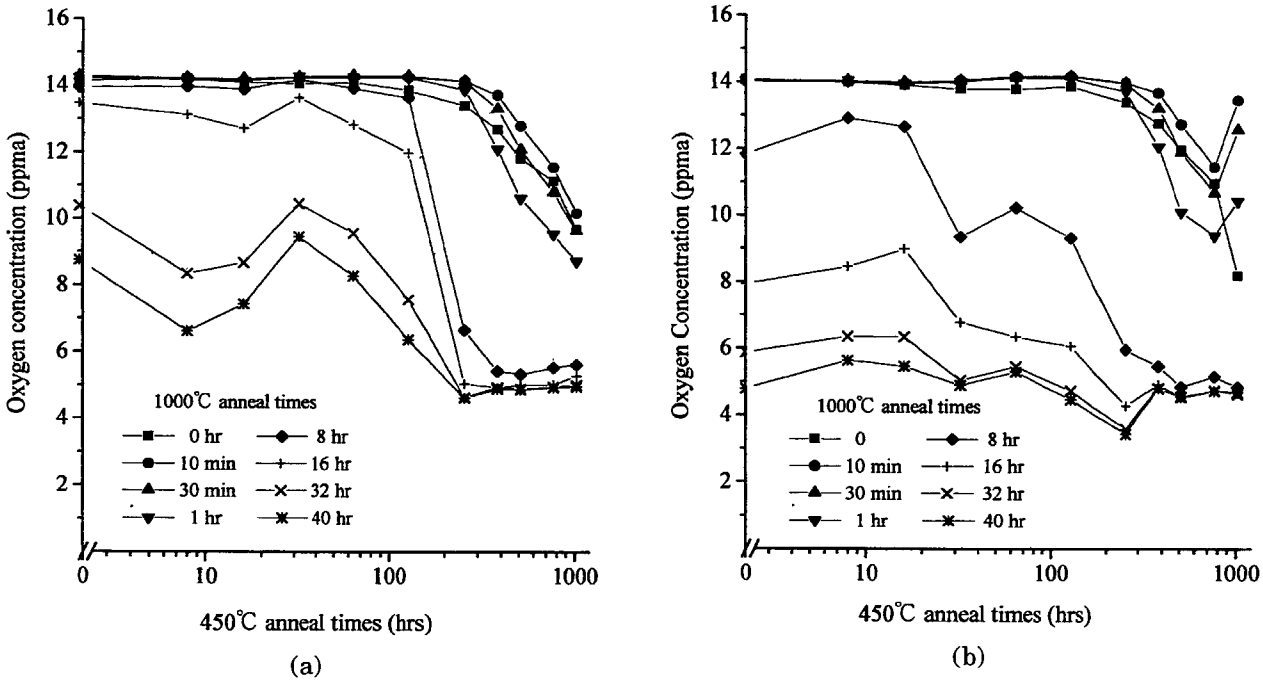

Fig. 1 Oxygen concentration after different growth anneal times at 1000℃ as a function of the nucleation anneal time at 450℃. (a) Two-step process. (b) Three-step process.

dissolution clearly occurs during short anneals (10 min and 30 min) at 1000℃, indicating that a large number of precipitate nuclei smaller than the critical size at 1000℃ are dissolved. For growth anneals up to 1 h at 1000℃, there is no difference between the two-step and three-step annealed wafers in terms of the oxygen concentration. However, for longer anneal times at this temperature, the three-step annealed samples always show lower post-anneal oxygen concentration than the two-step annealed samples at the same growth-anneal time, indicating that the 1-h anneal at 1150℃ enhances oxygen precipitation.

Figures 2 and 3 show optical photomicrographs of samples that received two-step and three-step anneals with a 40-h growth anneal at 1000℃. Four types of micro-etch pits have been observed in this research: 1) etch pit clusters; 2) dispersive pits, 3) paired pits and 4)long-shape pits. However, in the figures, only etch pit clusters (marked as C) and long-shape pits (marked as S.F.) can be easily identified; the high density of very tiny dispersive pits was not revealed in the optical photomicrographs. An example of paired pits is marked as D in the scanning electron micrograph of Fig. 4.

Compared with the TEM observations of by Patrick et al.[14,15] the etch pits described above are, respectively, 1) the pits of oxygen precipitate clusters tangled with dislocations, 2) dispersive precipitates, 3) dislocation loops, and 4) stacking faults possibly embedded with a few small precipitates. The micro-defect structures are not very different for two-step and three-step annealed samples with similar nucleation anneal times. In the samples annealed at 450℃ for short times, the majority of the defects are precipitate clusters and dispersive precipitates; few stacking faults are observed. At increased nucleation anneal times, the density of the precipitate clusters decreases while the density of stacking faults and dispersive

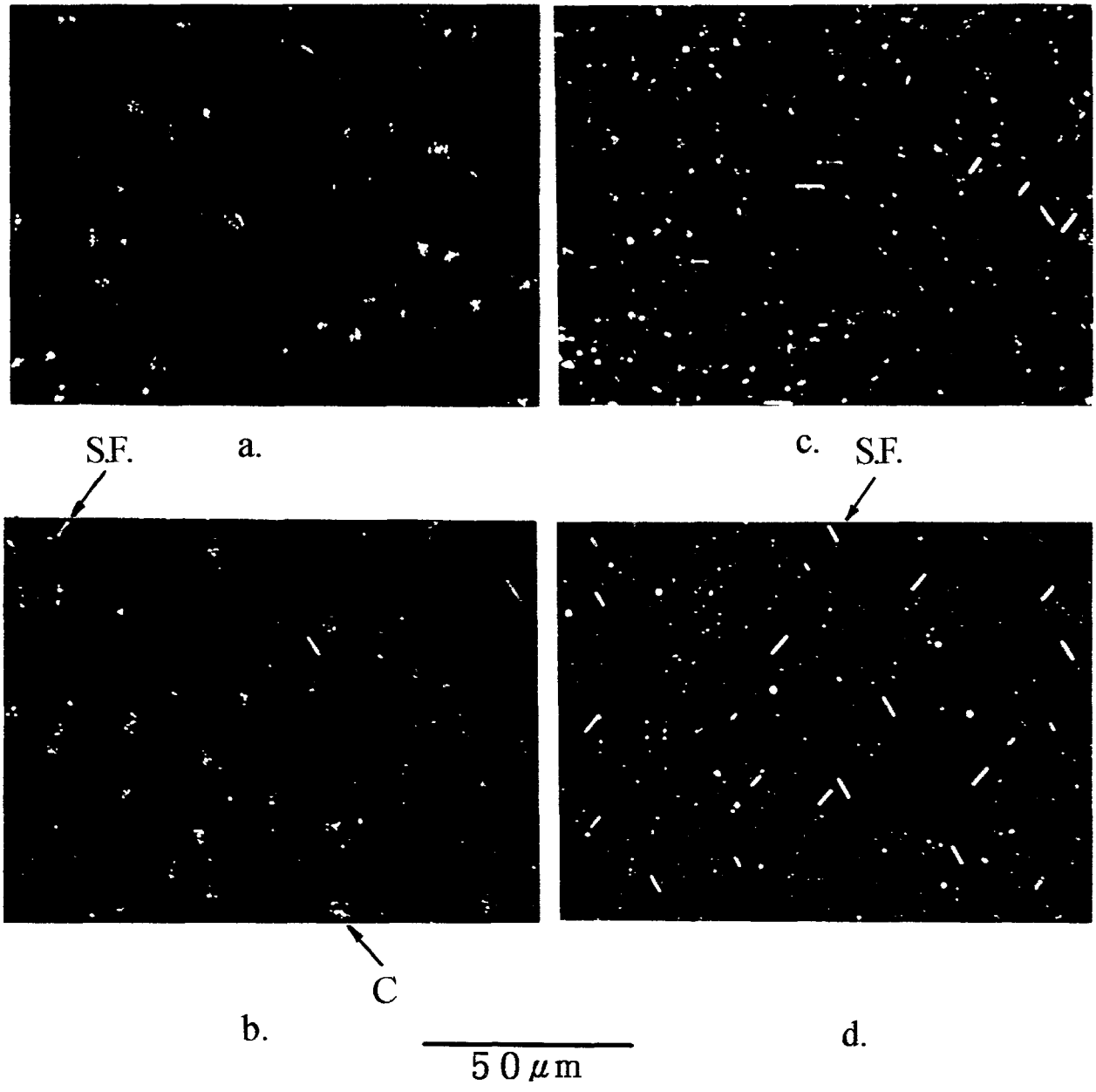

Fig. 2 Optical photomicrographs of wafer cross sections after a 40-h growth anneal at 1000°C preceded by nucleation annealing at 450°C for times of (a) 0 h, (b) 16 h, (c) 64 h, and (d) 128 h. Samples were Wright etched for about 3 min. to delineate the defects.

precipitates increases. At nucleation anneal times of 128 h and longer, the precipitate clusters nearly disappeared, and the density of stacking faults and dislocation loops increased rapidly. This trend can be seen in Fig. 4, which shows high densities of stacking faults and dislocation loops in a sample that had received a two-step anneal (256 h at 450°C followed by 40 h at 1000°C). In general, a higher density of stacking faults was observed in the three-step annealed samples than in the two-step annealed samples.

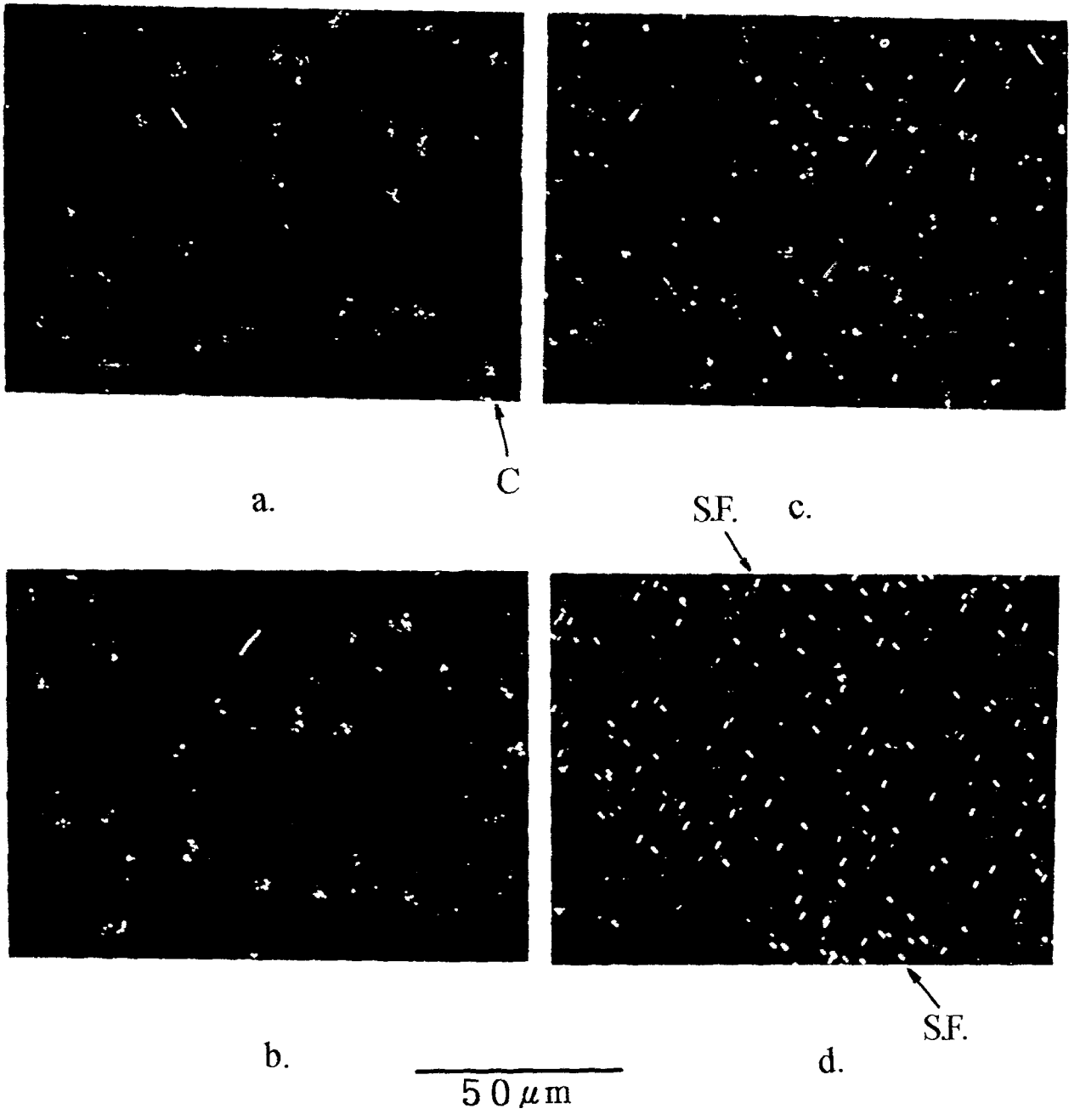

Fig. 3 Optical photomicrographs of wafer cross sections after a 40-h growth anneal at 1000℃ preceded by a 1-h pre-anneal at 1150℃ and nucleation annealing at 450℃ for times of (a) 0 h, (b) 16 h, (c) 64 h, and (d) 128 h. Samples were Wright etched for about 3 min. to delineate the defects.

Several models have been proposed to explain precipitation retardation. Kung[10] proposed a model based on the interaction between rod-likedefects and platelet precipitates to explain the differences between the results obtained during two-step and three-step annealing. In Kung's model, the nuclei of rod-like defects would be annealed out during the initial high temperature anneal in the three-step cycle. Therefore, fewer stacking faults would be generated in samples which received a prolonged 450℃ nucleation anneal in the three-step anneal test. Obviously, the microstructures

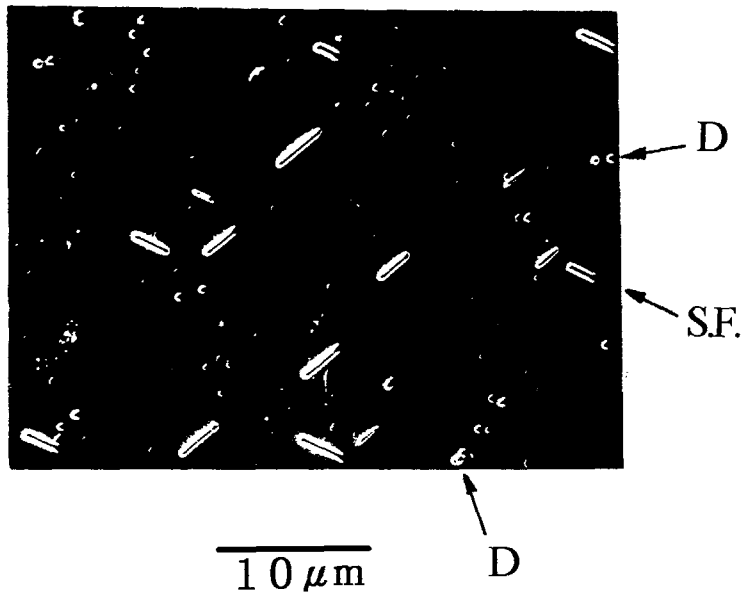

Fig. 4 A typical SEM photomicrograph of a wafer cross section after a 40-h growth anneal at 1000℃ preceded by nucleation annealing for a time longer than 256 h.

observed in the three-step anneal in the experiments reported here do not follow this model. It seems that the silicon interstitial (I) supersaturation model proposed by Tan and Kung [9] can best explain the results reported here. Tan and Kung suggested that when oxide precipitates grow fast enough, I-supersaturation would be easily reached and the growth of the smaller precipitates would be suppressed, thus causing precipitation retardation. When silicon interstitials accumulate to certain levels, rod-like defects or stacking faults start to nucleate, consequently reducing the silicon interstitial concentration in the sample. Then the growth of the smaller precipitates would no longer be suppressed and oxygen precipitation rate increases. In their model, the formation of a high density of stacking faults is necessary for precipitation recovery.

This model can also explain the three-step anneal results in this research, despite the fact that the nature of the defects formed in the silicon during the initial 1150℃ anneal is still unknown. The 1-h anneal at 1150℃ is observed to enhance oxygen precipitation growth. Therefore, interstitial supersaturation can be reached with shorter nucleation anneal times, resulting in earlier precipitation retardation. However, we suspect that the retardation in the three-step anneals may be due to different mechanisms; further research on this issue is continuing.

Since in the experiments reported here, none of the high temperature processes involved ramping scheme, the mechanism of the pronounced retardation effects observed in the two-step anneal test can not be associated with temperature ramping as previously suggested[11].

For nucleation anneal times longer than 256 h, the oxygen concentrations after growth anneal for 8 h at 1000℃ are close to the equilibrium value (about 3 ppma). Precipitation activity almost ceases during longer (16 h to 40 h) growth anneals at 1000℃. Less than 0.2 ppma oxygen was precipitated in this period. At this stage, samples annealed for 384 h or longer at 450℃ consistently revealed higher oxygen concentration than samples annealed for 256 h at this temperature. Again, longer nucleation anneal times result in a lower oxygen precipitation. These effects seem to suggest

the existence of another type of precipitation retardation. Similar results have also been observed during two-step (650℃-1000℃) and three-step (1150℃-650℃-1000℃) tests with identical samples described earlier in this paper (need reference here). The retardation observed in this region may be attributed to the Ostwald ripening effect. When the interstitial oxygen concentration reaches the saturation level, the growth of larger precipitates will dissolve the smaller ones and lead to precipitation retardation. When the 450℃ anneal time is long enough, more nuclei will grow to a size to coarsen the smaller ones during the 1000℃ growth anneal. In this experiment, we consistently observed a high density of stacking faults and dislocation loops, similar to those shown in Fig. 4, in the samples that received prolonged 450℃ nucleation anneals. The role played by the stacking faults in precipitation retardation in this region is an interesting topic.

4. SUMMARY

In this research, we carefully chose Cz silicon wafers with identical initial characteristics to run both 450℃-1000℃ two-step and 1150℃-450℃-1000℃ three-step anneal tests. No temperature ramping scheme was employed during any of the high temperature processing. A similar dependence of the microstructure characteristics on the 450℃ anneal time is observed for both the two-step and three-step annealed samples. However, a distinct retardation of precipitation is observed during the two-step anneal, while the retardation in the three-step anneal is less pronounced. The initial high temperature (1150℃) anneal in N_2 ambient in the three-step process induces precipitation retardation at an earlier nucleation stage. The precipitation retardation observed in this research is attributed to silicon interstitial supersaturation during low temperature annealing. The mechanisms associated with temperature ramping are shown not to be the major cause of the precipitation retardation. We also observed another type of precipitation retardation when the low temperature anneal time is longer than 256 h.

ACKNOWLEDGMENTS

This work was supported by the National Science Council of the Republic of China under Contract No. NSC84-2215-E005-004.

REFERENCES

1. T. Y. Tan, E. E. Gardner, and W. K. Tice, *Appl. Phys. Lett.* 30 (1977) 175.
2. H. Chiou, *Solid State Technol.* (1987) No. 3, 77.
3. K. Yamamoto, S. Kishino, Y. Matsushita, and T. Iizuka, *Appl. Phys. Lett.* 36 (1988) 195.
4. F. Shimura, H. Tsuya, and T. Kawamura, *J. Electrochem. Soc.* 128 (1981) 1579.
5. K. Nagasawa, Y. Matsushita, and S. Kishino, *Appl. Phys. Lett.* 37 (1980) 622.
6. S. Isomae, S. Aoki, and K. Watanabe, *J. Appl. Phys.* 55 (1984) 817.
7. M. Ogino, *Appl. Phys. Lett.* 41 (1982) 847.
8. C. Y. Kung, L. Forbes, and J. D. Peng, Defects in Silicon, eds. W. M. Bullis and L. C. Kimerling (*The Electrochemical Society, Pennington, N.J.,1983*) p.185.
9. T. Y. Tan and C. Y. Kung, *J. Appl. Phys.* 59 (1986) 917.
10. C.Y. Kung, Jpn. *J. Appl. Phys.* 31 (1992) 2846.
11. W.B. Rogers, H. Z. Massoud, R. B. Fair, U. M. Gosele, T. Y. Tan, and G. A. Rozgonyi, *J. Appl. Phys.* 65 (1989) 4215.
12. A. Bourrett J. Thibault-Desseaux, and D. N. Seidman, *J. Appl. Phys.* 55(1984) 825.
13. W. Bergholz, J. L. Hutchison, and {missing initial} Pirouz, *J. Appl.Phys.* 58 (1985) 3419.
14. M. Wright-jenkins , *J.Electrochem. Soc.* 124 (1977) 757.

15. W. Patrick, E. Hearn, and W. Westdorp, *J. Appl. Phys.* 50 (1979) 7156.
16. D.M.Maher, A. Staudinger, and J. R.Patel, *J. Appl.phys.* 47 (1976) 3813.

論文收稿日期：86年 1月14日
論文修訂日期：86年 2月20日
論文接受日期：86年 2月27日